# Glucose Intolerance and Lipid Metabolic Adaptations in Response to Intrauterine and Postnatal Calorie Restriction in Male Adult Rats

Meena Garg, Manikkavasagar Thamotharan, Yun Dai, Venu Lagishetty, Aleksey V. Matveyenko, W. N. Paul Lee, and Sherin U. Devaskar

Department of Pediatrics (M.G., M.T., Y.D., V.L., S.U.D.), Division of Neonatology and Developmental Biology, Neonatal Research Center, and Department of Medicine (A.V.M.), Division of Endocrinology, Larry L. Hillblom Islet Research Center, and David Geffen School of Medicine (M.G., M.T., Y.D., V.L., S.U.D., A.V.M.), University of California, Los Angeles, Los Angeles, California 90095-1752; and Department of Pediatrics (W.N.P.L.), Division of Endocrinology, Harbor-UCLA Medical Center, Torrance, California 90502

Enhanced *de novo* lipogenesis (DNL), an adult hepatic adaption, is seen with high carbohydrate or low-fat diets. We hypothesized that *ad libitum* intake after prenatal calorie restriction will result in adult-onset glucose intolerance and enhanced DNL with modified lipid metabolic gene expression profile. Stable isotopes were used in 15-month-old adult male rat offspring exposed to prenatal (IUGR), pre- and postnatal (IPGR), or postnatal (PNGR) caloric restriction *vs.* controls (CON). IUGR *vs.* CON were heavier with hepatomegaly but unchanged visceral white adipose tissue (WAT), glucose intolerant with reduced glucose-stimulated insulin secretion (GSIS), pancreatic $\beta$-cell mass, and total glucose clearance rate but unsuppressed hepatic glucose production. Liver glucose transporter (Glut) 1 and DNL increased with decreased hepatic acetyl-CoA carboxylase (ACC) and fatty acid synthase but increased WAT fatty acid transport protein-1 and peroxisomal proliferator-activated receptor-$\gamma$, resistin, and visfatin gene expression. In contrast, PNGR and IPGR were lighter, had reduced visceral WAT, and were glucose tolerant with unchanged hepatic glucose production but with increased GSIS, $\beta$-cell mass, glucose clearance rate, and WAT insulin receptor. Hepatic Glut1 and DNL were also increased in lean IPGR and PNGR with increased hepatic ACC, phosphorylated ACC, and pAMPK and reduced WAT fatty acid transport protein-1, peroxisomal proliferator-activated receptor-$\gamma$, and ACC$\alpha$. We conclude the following: 1) the heavy, glucose-intolerant and insulin-resistant IUGR adult phenotype is ameliorated by postnatal caloric restriction; 2) increased DNL paralleling hepatic Glut1 is a biomarker of exposure to early caloric restriction rather than the adult metabolic status; 3) hepatic lipid enzyme expression reflects GSIS rather than DNL; and 4) WAT gene expression reflects an obesogenic *vs.* lean phenotype. **(*Endocrinology* 154: 102–113, 2013)**

Nutritional programming of glucose kinetics in response to prenatal calorie restriction along with postnatal adaptations, predetermine the ultimate adult phenotype. Intrauterine growth restriction (IUGR) is associated with the development of adult metabolic syndrome with comorbidities including type 2 diabetes mellitus, obesity, hypertension, coronary heart disease, and dyslipidemia (1, 2).

In type 2 diabetes mellitus skeletal muscle, insulin resistance and its inability to store ingested glucose by glycogen synthesis are hypothesized to enhance hepatic glucose storage via *de novo* lipogenesis (DNL), thereby resulting in atherogenic dyslipidemia (3). We have, however, previously shown that the adult male IUGR rat offspring expresses adiposity while retaining total body in-

ISSN Print 0013-7227 ISSN Online 1945-7170
Printed in U.S.A.

doi: 10.1210/en.2012-1640 Received June 16, 2012. Accepted October 18, 2012.
First Published Online November 26, 2012

Abbreviations: ACC, Acetyl-CoA carboxylase; AIR, acute insulin response; AMPK, AMP kinase; $C_T$, cycle threshold; DI, disposition index; DNL, *de novo* lipogenesis; FAS, fatty acid synthase; FATP, fatty acid transport protein; FOXO, Forkhead box O; GC, glucose clearance; GC/MS, gas chromatography/mass spectrometry; Glut, glucose transporter; GSIS, glucose-stimulated insulin secretion; GTT, glucose tolerance test; HDL, high-density lipoprotein; HGP, hepatic glucose production; IR, insulin receptor; IUGR, intrauterine growth restriction; p, phosphor; IVGTT, iv GTT; PN, postnatal day; PPAR, peroxisomal proliferator-activated receptor; RBP4, retinol binding protein 4; SCD, stearoyl-coenzyme A-desaturase; $S_I$, insulin sensitivity; Sirt, Sirtuin; SREBP, sterol regulatory element-binding protein; UC, unesterified cholesterol; WAT, white adipose tissue.

sulin sensitivity (4). Fatty liver in the IUGR rat offspring is evident during fetal and newborn life before the onset of adult obesity (5). Hepatic DNL contributes toward development of fatty liver in genetically engineered mouse models (6). In the adult IUGR rat offspring with reported upregulated lipogenic transcription factor [sterol regulatory element-binding protein (SREBP)-1c] and enzyme fatty acid synthase (FAS) expression suggest increased hepatic lipogenesis (7), although this function has never been examined.

In contrast, human and animal adult studies with increased dietary carbohydrates, low dietary fat or calorie restriction are also known to increase DNL (8). Although hyperglycemia with hyperinsulinemia are known to enhance lipogenic enzyme gene expression responsible for DNL (9), high-fat or cafeteria diets, activation of energy sensing AMP kinase (AMPK) to phosphor (p) AMPK, or increased lipid and energy sensing Sirtuin (Sirt)-1 generally decrease DNL (9–12).

Enhanced DNL is one of the consequences of insulin resistance, which in turn leads to obesity in adult mice and humans (13). Whether DNL plays such a role in development of an obesogenic phenotype with a fatty liver of the adult IUGR offspring exposed to pre- or postnatal caloric restriction is not known. We hypothesized that prenatal calorie restriction with or without subsequent postnatal calorie restriction will enhance DNL in the adult male offspring. We tested this hypothesis in a rat model of pre- and postnatal calorie restriction described previously by us (4).

## Materials and Methods

### Animals

Sprague Dawley rats (Charles River Laboratories, Hollister, CA) were housed in individual cages, exposed to 12-h light, 12-h dark cycles at 21-23 C and allowed *ad libitum* access to standard rat chow (NIH-31 modified 6% mouse/rat sterilizable diet 7013, composition of carbohydrate 63.9%, fat 6%, and protein 14.5%; Harlan, Teklad, CA). The National Institutes of Health guidelines were followed as approved by the Animal Research Committee of the University of California, Los Angeles.

### Animal model

We provided 50% of daily food intake (11 g/d) of a pregnant Sprague Dawley rat with *ad libitum* access to water from embryonic d 11 to embryonic d 21 as previously described by us (4). This prenatal seminutrient restriction led to IUGR (4). At birth, the litter size was culled to six to ensure no interlitter nutritional variability. Postnatally the cross-fostering of pups generated four experimental groups as previously described by us (4). The newborn pups born to *ad libitum*-fed control mothers were reared by either mothers continued on semicaloric restriction from postnatal day (PN) 1-PN21 [postnatal caloric restriction alone (PNGR)] or by control mothers (CON) (Supplemental Fig. 1, published on The Endocrine Society's Journals Online web site at http://endo.endojournals.org). During the suckling phase, the intrauterine semi-calorie-restricted progeny was fed either by control mothers with *ad libitum* access to nutrients (IUGR) representing intrauterine caloric restriction or by semi-calorie-restricted mothers that continued to receive 50% of daily food intake (IPGR) representing intrauterine and postnatal caloric restriction. The offspring were maintained until 15 months of age at which time the males were studied. After all the *in vivo* investigations and after measuring body weight, animals were euthanized, and organs/tissues (brain, heart, liver, pancreas, kidneys, white adipose tissue, and brown adipose tissue) were removed and weighed individually.

### Intravenous glucose tolerance test (GTT)

Fifteen-month-old adult male awake animals (n = 13) received 1 g/kg body weight of the 1:1 mixture of [2-$^2$H] and [6,6-$^2H_2$]glucose (>98% pure; Cambridge Isotope Laboratories, Andover, MA) via surgically placed jugular venous catheters (14). Blood (500 $\mu$l) was obtained at 0, 5, 15, 30, 45, 60, and 120 min for assessment of hormone and glucose concentrations, and isotopomer enrichment (n = 5 in CON and n = 4 in each of the other three groups).

### Measurement of DNL

Animals from each group (n = 23 total) received 0.09% NaCl in 99.9% $D_2O$ (ip) equal to approximately 2% of body weight at the beginning of the study. Animals had free access to drinking water containing 6% $D_2O$ (99.9% deuterium; Cambridge Isotope Laboratories, Andover, MA). Food and water intake was measured over a 24-h period, taking into account food spillage and evaporation, daily for 7 d of the experiment and averaged. Tail vein blood samples were collected at baseline and subsequently on d 2, 4, 6, and 8 (Supplemental Fig. 2). Plasma enrichment of deuterium was comparable in all groups at 3% by d 8 of the experiment (Supplemental Fig. 2). Serum was separated and kept frozen at −80 C for gas chromatography/mass spectrometry (GC/MS) analysis. Fatty acid extraction was performed using methods described by Lowenstein *et al.* (15). Plasma samples (50 $\mu$l) were saponified in 200 proof ethanol and 30% KOH (wt/vol) in a 1:1 volume overnight at 70 C. Samples were acidified with HCl, and fatty acids were extracted three times with petroleum ether and air dried. Fatty acids were derivatized as methyl esters using 0.5 N methanolic HCl, dried under a nitrogen stream, and subsequently reconstituted with hexane for GC/MS analysis.

### Gas chromatography/mass spectrometry analysis

GC/MS was performed on a Hewlett-Packard model 5973 mass selective detector connected to a model 6890 gas chromatograph (Hewlett-Packard, Palo Alto, CA).

#### *Glucose*

Glucose was analyzed by GC/MS using a modified method described by Szafranek *et al.* (16). Electron impact ionization was used to determine glucose isotopomers of [6,6-$2H_2$]glucose at a mass to charge ratio of 187 for C3-C6 and [2-$^2$H]glucose at a mass to charge ratio 242 for C1-C4 fragments (14, 17). Mass isotopomer distribution was determined using the method of Lee

*et al.* (18). The disappearance of the two isotopes, [2-$^2$H]- and [6,6-2$H_2$]glucose was determined as the M1 label for [2-$^2$H] glucose and the M2 label for [6,6-2$H_2$]glucose (14, 19). The difference between the disappearance rates of M1 and M2 was used as a measure of futile cycling (*i.e.* glucose to glucose-6-phosphate and back) (19). Unsuppressed endogenous hepatic glucose production during GTT was derived from the increase in unlabeled glucose concentration M0, which was assessed by subtracting the labeled glucose fraction from the total glucose concentration.

### *Fatty acids*

Fatty acids were analyzed as their methyl esters after derivatization. Palmitate and stearate were separated on the gas chromatograph with a glass capillary column BPX70 (SGE, Austin, TX) measuring 30 m × 250 μm (inner diameter). Mass isotopomer distribution was determined using the method of Lee *et al.* (20). The major peaks in the ion chromatogram are the long-chain fatty acids palmitate (c16:0), stearate (c18:0), oleate (c18:1, *cis*), and elaidate (c18:1, *trans*). The area under each peak was integrated using the Agilent ChemStation software (Newtown, PA). The fraction of new synthesis representing DNL = ME (fatty acid)/(p × N), in which ME (molar enrichment) is the average number of deuterium atoms incorporated per molecule calculated from mass isotopomer distribution, p is the deuterium enrichment (specific activity) in water, which is determined using the m2 to m1 consecutive mass isotopomer ratio, and N is the number of deuterium per molecules incorporated from body water per molecule of fatty acid (*e.g.* Ref. 21 for palmitate) (20-22).

## Plasma assays

Plasma was separated and aliquots stored at −20 C for measurement of glucose by the glucose oxidase method (Sigma Diagnostics, St. Louis, MO; sensitivity = 0.1 mM). Insulin, leptin, and adiponectin were quantified by ELISAs using rat standards and antirat insulin, leptin, or adiponectin antibodies (Linco Research Inc., St. Charles, MO; sensitivity: insulin and adiponectin = 0.2 ng/ml, leptin = 0.04 ng/ml, using 10 μl samples). The intraassay and interassay coefficient of variation was 6.5 ± 0.9%. Serum triacylglycerol, cholesterol, high-density lipoprotein (HDL) (23), unesterified cholesterol (UC), and free fatty acids were measured by colorimetric assays in triplicates (24).

## Hepatic insulin sensitivity ($S_I$) and disposition index (DI)

$S_I$ was calculated as 1/(endogenous glucose production × basal insulin concentration). DI was calculated from $S_I$ and acute insulin response (AIR) 5 min after an iv glucose bolus during the iv GTT (IVGTT) as a measure of whole body insulin sensitivity (25).

## Pancreatic β-cell mass

To quantify β-cell mass, the pancreas was rapidly removed from euthanized rats, weighed, and immediately fixed in 4% paraformaldehyde overnight at 4 C. The pancreas was embedded in paraffin, and subsequently complete longitudinal sections (4 μm) of pancreas (head, body, and tail) were obtained through their maximal width. Paraffin-embedded pancreatic sections were subsequently stained first for hematoxylin/eosin and insulin (guinea pig antiinsulin, 1:100; Zymed, Carlsbad, CA), and β-cell mass was measured by first quantifying the pancreatic cross-sectional area positive for insulin and multiplying this by the pancreatic weight. Images were acquired using OpenLab 5 software (Improvision, PerkinElmer, Waltham, MA) and analyzed using ImagePro Plus software (Media Cybernetics, Inc., Rockville, MD).

## Hepatic and white adipose tissue (WAT) lipid metabolic enzyme, insulin receptor (IR) and glucose transporter (Glut) protein expression

### *Antibodies*

Mouse anti-FAS was purchased from BD Transduction Laboratories. Rabbit antiacetyl-CoA carboxylase (ACC), anti-p-ACC, AMPKα, p-AMPKα, and IR-β subunit were from Cell Signaling (Danvers, MA). Anti-Glut2 antibody was purchased from Millipore (Temecula, CA). Antivinculin antibody was obtained from Sigma Chemical Co. (St. Louis, MO). Anti-Glut1 and Glut4 antibodies were produced and characterized as previously described by us (26, 27).

### *Western blot analysis*

Liver and visceral WAT homogenates were subjected to Western blot analysis as previously described (27, 28). Primary antibody (1:500 dilution for FAS, ACC, and p-ACC and 1:1000 for AMPKα, p-AMPKα, IR-β subunit, Glut1, Glut2, and Glut4) incubations were overnight at 4 C. The quantification of protein bands was performed by densitometry using the Scion Image software (Frederick, MD). Protein band density in arbitrary units was normalized to vinculin (internal control) and expressed as a percent of CON values.

## WAT mRNA expression by RT-PCR

Expression of adipokines, transcription factors, or transporters/enzymes in WAT (see Table 4) were analyzed first by RT-PCR and in some cases real-time PCR was used for quantification (27, 28). Primer sequences, gene accession codes, optimal annealing temperatures, and the number of cycles employed are shown in Supplemental Table 1. The 18S mRNA gene was used as the internal control. Comparative (Δ) cycle threshold ($C_T$) method in which $C_T$ is the threshold cycle number was used for quantification and the difference in threshold cycles for the target and the internal control genes was then normalized relative to that of the CON group by $2^{-\Delta\Delta CT}$.

## Statistical analysis

All data are expressed as mean ± SE. The ANOVA models were used on normally distributed data to compare various treatment groups at different ages and F values determined. The intergroup differences were determined by the Fisher's paired least significance difference test when ANOVA revealed significance. Significance levels were computed on the basis of exact methods accounting for the small sample size, and $P < 0.05$ was assigned significance.

# Results

## Anthropometric measurements, food and water intake, plasma glucose, and hormone concentrations

At birth IUGR and IPGR weighed less than CON (Table 1). At 15 months of age, IUGR males were signif-

**TABLE 1.** Body weight, food and water intake corrected for body weight, and plasma glucose and hormone concentrations for all groups are shown as mean ± SEM

| | CON | IUGR | IPGR | PNGR |
|---|---|---|---|---|
| Birth weight (g) (n = 15) | 7.5 ± 0.5 | 5.32 ± 0.4[a] | 5.88 ± 0.8[a] | 8.1 ± 0.9 |
| 21-d weight (g) (n = 15) | 62.6 ± 4 | 55.4 ± 3.6 | 25.3 ± 1.1[a,b] | 26.3 ± 1.6[a,b] |
| 15-month weight (g) (n = 15) | 895.7 ± 36.9 | 989.8 ± 34.3[a,c,d] | 756.3 ± 28.8[a,b] | 741.7 ± 15.7[a,b] |
| Food intake (g/d) (n = 15) | 26.1 ± 1.8 | 32.6 ± 1.7[a,c,d] | 24.8 ± 1.8[a,b] | 24.3 ± 1.8[a,b] |
| Water intake (g/d) (n = 15) | 37.4 ± 2.1 | 44.7 ± 4.1 | 33.5 ± 1.8 | 34.9 ± 1 |
| Food intake (g/g body weight) (n = 15) | 0.029 ± 0.002 | 0.034 ± 0.002 | 0.033 ± 0.002 | 0.033 ± 0.002 |
| Water intake (g/g body weight) (n = 15) | 0.042 ± 0.001 | 0.048 ± 0.007 | 0.046 ± 0.002 | 0.048 ± 0.002 |
| Plasma glucose (mg/dl) (n = 10) | 122.8 ± 5.3 | 163.1 ± 3.8[a] | 134.7 ± 14.3 | 132.6 ± 5.6 |
| Plasma insulin (ng/ml) (n = 10) | 1.6 ± 0.3 | 1.8 ± 0.4 | 2.1 ± 0.3[c] | 1.3 ± 0.2 |
| Plasma leptin (ng/ml) (n = 10) | 30.2 ± 3.4 | 27.6 ± 4.4 | 15.2 ± 1.9[a,b] | 18.3 ± 1.9[a,b] |
| Plasma adiponectin (ng/ml) (n = 8) | 10.0 ± 1.0 | 8.7 ± 1.7 | 11.2 ± 1.7 | 12.8 ± 3.5 |

Number of animals for each parameter is shown in *parentheses* (n).

[a] $P < 0.05$ all groups *vs.* CON.

[b] $P < 0.05$ *vs.* IUGR.

[c] $P < 0.05$ *vs.* IPGR.

[d] $P < 0.05$ *vs.* PNGR.

icantly heavier with hepatomegaly and hyperglycemic under basal conditions after overnight fast when compared with CON (Tables 1 and 2). WAT weights and leptin concentrations were no different in IUGR from CON (Tables 1 and 2). The IPGR and PNGR groups were significantly lighter with lower plasma leptin concentrations compared with CON (Table 1). The IPGR and PNGR groups had significantly lower pancreatic and WAT weights *vs.* CON (Table 2). There was no difference in food and water intake per unit body weight between groups (Table 1). However, total daily water intake (grams per day) was significantly higher in the IUGR group compared with the IPGR (10% less than CON) and PNGR (7% less than CON) groups with a tendency toward an increase compared with CON (19% more) (Table 1). Similarly total food intake (grams per day) was increased in IUGR compared with CON (by 25%), IPGR (by 5%), and PNGR (by 7%). The basal plasma insulin and adiponectin concentrations in the experimental groups were not significantly different from CON (Table 1).

### GTT and glucose-stimulated insulin secretion (GSIS)

IUGR were hyperglycemic in the second phase of IVGTT with increased plasma glucose concentrations at 60 and 120 min after the glucose challenge (Fig. 1A) and increased glucose area under the curve compared with IPGR and PNGR with an increased trend *vs.* that of CON (Fig. 1A, *inset*). This hyperglycemia in IUGR reflected the deficiency of GSIS in the first and second phases of IVGTT (Fig. 1B). PNGR and IPGR were glucose tolerant similar to CON (Fig. 1A and the *respective inset*). IPGR remained euglycemic due to hyperinsulinemia with increased first- and second-phase insulin response when compared with IUGR (Fig. 1B). IPGR and PNGR demonstrated the highest plasma insulin concentrations at 5 min, which were significantly greater than IUGR ($P < 0.05$ and $P < 0.006$, respectively; Fig. 1B). This insulin response was sustained in IPGR and significantly greater than PNGR at 60 ($P < 0.009$) and 120 ($P < 0.01$) min and greater than CON at 120 min ($P < 0.01$) only. Initial 5-min GSIS in PNGR

**TABLE 2.** Organ weights (grams) and nose-tail (N-T) length (centimeters) are shown for all groups as mean ± SEM

| | CON (15) | IUGR (16) | IPGR (15) | PNGR (15) |
|---|---|---|---|---|
| N-T length | 52 ± 0.3 | 51.6 ± 0.5 | 51.4 ± 0.4 | 51.9 ± 0.3 |
| Heart | 2.7 ± 0.1 | 2.4 ± 0.2 | 2.3 ± 0.1 | 2.5 ± 0.2 |
| Liver | 22.8 ± 1.2 | 24.1 ± 0.8[a,b] | 21.2 ± 0.8[c] | 21.7 ± 1.2 |
| Pancreas | 2.0 ± 0.2 | 1.6 ± 0.2 | 1.3 ± 0.1[a] | 1.5 ± 0.1[a] |
| Kidney | 5.0 ± 0.3 | 5.3 ± 0.6 | 4.4 ± 0.1[c] | 4.9 ± 0.2 |
| White adipose tissue | 42.4 ± 3.8 | 42.6 ± 3.1[b] | 23.3 ± 1.2[a,c] | 25.8 ± 3.2[a,c] |
| Brown adipose tissue | 1.0 ± 0.2 | 1.3 ± 0.2 | 1.1 ± 0.1 | 1.1 ± 0.2 |

Number of animals for each parameter is shown in *parentheses* (n).

[a] $P < 0.05$ all groups *vs.* CON.

[b] $P < 0.05$ *vs.* IPGR.

[c] $P < 0.05$ *vs.* IUGR.

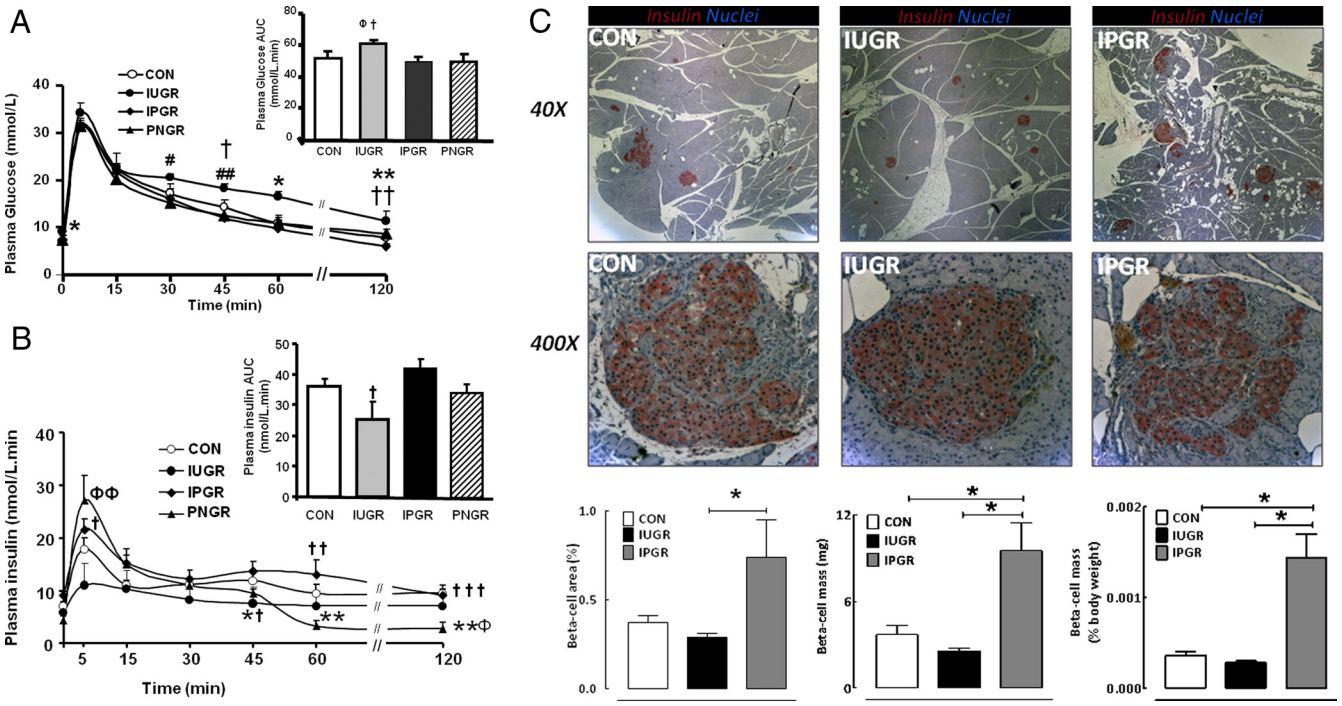


**FIG. 1.** Glucose tolerance tests and pancreatic β-cell morphology: A, Plasma glucose concentration during GTT at all time points after glucose challenge is shown. The *inset* depicts area under the curve (AUC) for plasma glucose concentration during the GTT for CON (n = 5), IUGR, PNGR, and IPGR (n = 4 each for the other groups). *, $P < 0.02$ IUGR *vs.* CON, IPGR, and PNGR; **, $P < 0.05$ IUGR *vs.* CON and IPGR; #, $P < 0.05$ IUGR *vs.* PNGR; ##, $P < 0.03$ IUGR *vs.* PNGR; †, $P < 0.05$ IUGR *vs.* IPGR; ††, $P < 0.006$ IUGR *vs.* IPGR; ϕ, $P < 0.05$ IUGR *vs.* PNGR. B, Plasma insulin concentrations during GTT at all time points after glucose challenge is shown. The *inset* depicts area under the curve (AUC) for plasma insulin in CON (n = 5), IUGR, IPGR, and PNGR (n = 4 each in all other groups). ϕ, $P < 0.05$; ϕϕ, $P < 0.006$ IUGR *vs.* PNGR; †, $P < 0.05$; ††, $P < 0.009$; †††, $P < 0.02$ IPGR *vs.* IUGR; *, $P < 0.03$; **, $P < 0.02$ PNGR *vs.* CON. C, Pancreatic β-cell morphology. Longitudinal sections of pancreas (magnification, ×40, *upper panels*, ×400, *middle panels*) from CON (*left panels*), IUGR (*center panels*), and IPGR (*right panels*) demonstrate β-cells stained for insulin (*pink*) and the 4′,6′-diamino-2-phenylindole nuclear stain (*blue*). The *lower panel* contains the corresponding quantification seen as bar graphs depicting β-cell area (as a percent of total pancreatic area) (*left panel*), β-cell mass (*center panel*), and β-cell mass corrected as a percent of body weight (*right panel*) (n = 4 per group). *, $P < 0.05$ between groups identified with a *horizontal line*.

reflected that of CON and IPGR, but GSIS was not sustained in the second phase of IVGTT (Fig. 1B). Area under the curve revealed a significant difference between IUGR and IPGR ($P < 0.04$) (Fig. 1B, *inset*).

## Pancreatic β-cell characteristics

Pancreatic β-cell fractional area and mass appeared reduced but was not statistically significant in IUGR when compared with CON (Fig. 1C). On the other hand, β-cell fractional area and mass were significantly higher in IPGR compared with CON and IUGR (3.7 ± 0.6 and 2.6 ± 0.2 *vs.* 9.5 ± 1.9 mg for CON and IUGR *vs.* IPGR, $P < 0.05$; Fig. 1C). Body weight-adjusted β-cell mass trended toward a reduction in IUGR *vs.* CON and was further increased in IPGR compared with CON and IUGR ($P < 0.05$; Fig. 1C).

## Glucose metabolic adaptations: endogenous hepatic glucose production (HGP), hepatic glucose recycling, and glucose clearance (GC) with hepatic and WAT Gluts and IR

### *Hepatic glucose production and recycling*

During IVGTT, IUGR demonstrated unsuppressed HGP ($P < 0.05$) (Fig. 2A) compared with CON in keeping with deficient GSIS in the first and second phase of IVGTT (Fig. 1B). PNGR and IPGR demonstrated suppression of HGP similar to CON (Fig. 2A). Percent contribution of recycled hepatic glucose toward the glucose turnover was 63 ± 6.1% in CON, which was not significantly different from that of IUGR (60.2 ± 8.7), IPGR (55.4 ± 9.8), or PNGR (55.4 ± 6.0).

### *Hepatic Gluts (Glut2 and Glut1) and IR*

Changes in HGP during GTT were associated with no change in hepatic Glut2 (adult liver isoform; mediates bidirectional hepatocyte glucose transport) in any of the experimental groups but an increase in Glut1 (fetal/neonatal type; mediates unidirectional periportal intrahepatocyte glucose transport) protein concentrations in IUGR ($P = 0.02$), IPGR ($P = 0.01$), and PNGR ($P = 0.03$) *vs.* CON (Fig. 2B). Furthermore, no interexperimental group difference in hepatic IR (β-subunit mediates insulin action) concentration was observed (Fig. 2C).

### *Glucose clearance*

Whole-body GC was decreased in IUGR, with no change observed in IPGR but an increase in PNGR (Fig.

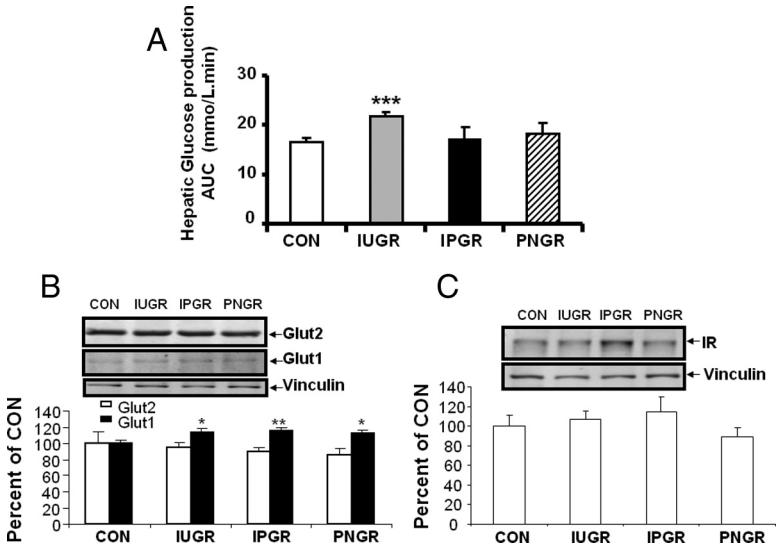


**FIG. 2.** Hepatic studies. A, Hepatic glucose production. Area under the curve (AUC) for endogenous hepatic glucose production (M0) during glucose tolerance test CON (n = 5), IUGR, PNGR, and IPGR (n = 4 each in all other groups). ***, $P < 0.04$ IUGR *vs.* CON. B, Hepatic glucose transporters. Representative Western blots demonstrating Glut2 (*upper panel*), Glut1 (*middle panel*), and vinculin (*lower panel*) as the internal control are seen in the *inset*. Quantification is shown as the bar graph below with results depicted as a percent of CON in arbitrary units (n = 6 in each group for each protein). *, $P < 0.02$, <0.03; **, $P < 0.01$ *vs.* CON. C, Hepatic insulin receptor. Representative Western blots are shown in the *inset* demonstrating IR β-subunit (*upper panel*) and vinculin (*lower panel*) as the internal control. Quantification is shown as the bar graph below with results depicted as a percent of CON in arbitrary units (n = 6 in each group for each protein).

3A) when compared with CON. Basal $S_I$ trended to be lower in IUGR, 3-fold higher in IPGR ($P < 0.05$ *vs.* PNGR), with no change in PNGR when compared with CON (Fig. 3B). The DI, based on $S_I$ and GSIS, was no different in IUGR with a tendency toward a reduction in PNGR *vs.* CON. On the other hand, a significant increase in IPGR was observed when compared with CON, IUGR, and PNGR (Fig. 3B).

### *WAT Gluts (Glut4 and Glut1) and IR*

These results were associated with no change in WAT Glut4 (demonstrates insulin responsive translocation to the plasma membrane) concentrations in all four experimental groups (Fig. 3C); however, a trend toward an increase in Glut1 (mediates basal intracellular glucose transport) concentrations ($P = 0.07$, not significant) (Fig. 3C) with a statistically significant increase in IR concentrations ($P = 0.04$) (Fig. 3D) in IPGR *vs.* CON was observed.

## Hepatic DNL and hepatic enzyme expression

Although there were no differences in basal plasma lipid profile between the four experimental groups, triglycerides, total cholesterol, HDL, and free fatty acids when normalized to the AIR were significantly increased in IUGR when compared with CON, IPGR, and PNGR (Table 3). *De novo* synthesis of palmitate and stearate was significantly increased in IUGR, IPGR, and PNGR *vs.* CON (Fig. 4A). Palmitate synthesis was increased by approximately 9% in IUGR, approximately 10% in IPGR, and approximately 5% in PNGR *vs.* that of CON, supporting a 2-fold increase in DNL (palmitate synthesis) in response to prenatal caloric restriction (IUGR, IPGR) *vs.* PNGR. Representative Western blots and quantification of hepatic enzymes, ACC, pACC and FAS, which catalyze DNL are shown in all experimental groups (Fig. 4B). IUGR demonstrated decreased hepatic ACC and FAS protein concentrations (Fig. 4B). DNL was also increased in IPGR and PNGR (Fig. 4A), with increased hepatic ACC and pACC (Fig. 4B). Representative Western blots and quantification of Sirt1 and pAMPK that are known to decrease DNL are depicted in all experimental groups (Fig. 4C). There was no significant difference in sirt1 protein concentrations between the four groups, although trending toward an increase in IUGR, IPGR, and PNGR (Fig. 4C); however, pAMPK concentrations were increased in IPGR and PNGR, supporting the low hepatic cellular energy status (Fig. 4C). Thus, the enhanced DNL seen in IUGR, IPGR, and PNGR did not reflect the respective hepatic lipid enzyme profile encountered in the adult offspring. Instead, FAS protein concentrations reflected the observed GSIS (Fig. 1B), given that FAS is induced by insulin. A direct association was seen between GSIS and hepatic FAS (r value = 0.21, $P < 0.0001$) and ACC (r value = 0.3, $P < 0.0001$) protein concentrations.

## WAT genes, factors, and adipokines

### *Genes mediating FAS*

IUGR exhibited increased expression of genes mediating fatty acid synthesis in WAT, whereas it was decreased in IPGR and PNGR (Table 4). Compared with CON, fatty acid transport protein (FATP)-1 (52% of CON in IPGR and PNGR, $P < 0.05$ each), ACCα (39.3% of CON in IPGR and 56.0% of CON in PNGR, $P < 0.05$ each), peroxisomal proliferator-activated receptor (PPAR)-γ (72-82% of CON in IPGR and PNGR, $P < 0.05$ each), and Forkhead box O (FOXO)-1 (45% of CON in IPGR and PNGR, $P < 0.05$ each) exhibited decreased expression in IPGR and PNGR. This was suggestive of reduction in mechanisms mediating fatty acid synthesis in IPGR and PNGR compared with CON. In contrast in IUGR, FATP1 was significantly increased (1.5-fold, $P < 0.05$), with PPARγ (1.2-fold, $P > 0.05$) and FOXO1 (1.2-fold, $P >$

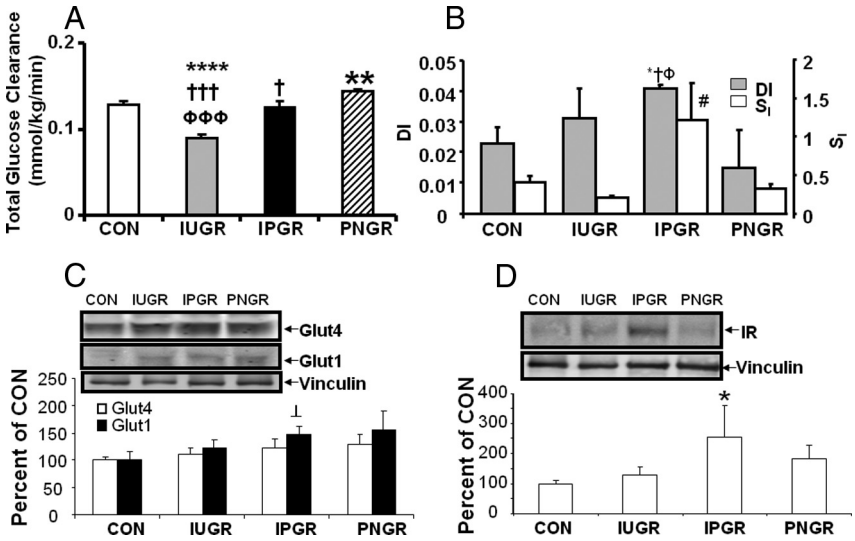


**FIG. 3.** Glucose clearance, insulin sensitivity, and WAT studies. A, Glucose clearance. Total glucose clearance during GTT is shown in CON (n = 5), IUGR, PNGR, and IPGR (n = 4 in all the other groups). ****, $P < 0.0002$, IUGR *vs.* CON; $\phi\phi\phi$, $P < 0.001$, IUGR *vs.* PNGR; †††, $P < 0.003$, IUGR *vs.* IPGR; †, $P < 0.05$, IPGR *vs.* PNGR; **, $P < 0.03$, PNGR *vs.* CON. B, Disposition index (DI = AIR, 5 min after glucose challenge × $S_I$) and $S_I$ [$S_I$ = 1/(basal hepatic glucose production × basal insulin concentration)rsqb] is depicted in CON (n = 5), IUGR, PNGR, and IPGR (n = 4 in all the other groups). *, $P < 0.03$, IUGR *vs.* CON; †, $P < 0.01$, IPGR *vs.* IUGR; $\phi$, $P < 0.02$, IPGR *vs.* PNGR; #, $P < 0.05$, IPGR *vs.* PNGR. C, WAT glucose transporters. Representative Western blots demonstrating Glut4 (*upper panel*), Glut1 (*middle panel*), and vinculin (*lower panel*) as the internal control are seen in the *inset*. Quantification is shown as the bar graph below with results depicted as a percentage of CON in arbitrary units (n = 6 in each group for each protein). ⊥, $P = 0.07$ (not significant) *vs.* CON. D, WAT IR. Representative Western blots are shown in the *inset* demonstrating IR $\beta$-subunit (*upper panel*) and vinculin (*lower panel*) as the internal control. Quantification is shown as the bar graph below with results depicted as a percentage of CON in arbitrary units (n = 6 in each group for each protein). *, $P = 0.04$ *vs.* CON.

0.05) not being different, albeit with a tendency toward an increase compared with CON, again suggesting a propensity of mechanisms mediating fatty acid transport and synthesis to be enhanced in IUGR *vs.* CON. Additionally, unlike the hepatic enzyme protein concentrations, GSIS was reciprocally associated with WAT FAS (r value = $-0.3$, $P < 0.001$) and ACC (r value = $-0.21$, $P < 0.0003$) expression. The expression of SREBP1 and SREBP2, transcription factors regulating genes that mediate fatty acid synthesis, were not altered by pre- and/or postnatal calorie restriction.

### *Factors associated with FAS*

Sirt1, a nicotinamide adenine dinucleotide oxidase-dependent protein deacetylase known to regulate FOXO1 transcription, is an important regulator of energy homeostasis in response to nutrient availability (29). Decreased expression of Sirt1 in WAT (63% of CON in IPGR and PNGR, $P < 0.05$ each) was consistent with the observed decreased expression of WAT FOXO1 in IPGR and PNGR ($P < 0.05$ each). Retinol binding protein 4 (RBP4), a cytokine linked to insulin resistance and obesity, demonstrated reduced expression in IPGR (55.1% of CON, $P < 0.05$) and PNGR (58.7% of CON, $P < 0.05$), consistent with the observed decreased fat content in these groups. Stearoyl-coenzyme A-desaturase (SCD)-1, a key and highly regulated enzyme that is required for biosynthesis of monounsaturated fatty acids, catalyzes the D9-cis desaturation of a range of fatty acyl-CoA substrates. SCD1 expression, although trending toward an increase in IUGR, IPGR, and PNGR, was not statistically different (Table 4).

### *Adipokines*

Adipocytokines such as resistin, visfatin, leptin, adiponutrin, TNF-$\alpha$, and adiponectin have been displayed to have significant roles in the development of obesity and insulin resistance. Resistin mRNA expression was increased in IUGR (1.7-fold), PNGR (1.5-fold) and IPGR (1.2-fold) compared with that of CON ($P < 0.05$ each). Visfatin mRNA expression was increased in IUGR (3.1-fold) and PNGR (2.8-fold) compared with that of CON ($P < 0.05$ each). Leptin mRNA was also increased in PNGR (1.8-fold) and IPGR (1.4-fold) compared with CON ($P < 0.05$) as assessed by both semiquantitative and real-time PCR. Adiponutrin mRNA concentrations, on the other hand, were decreased in IPGR (65.0% of CON) and PNGR (72.0% of CON) compared with CON ($P < 0.05$ each). TNF-$\alpha$ and adiponectin expression was comparable among the four groups ($P > 0.05$), with the former expressing an increasing trend in IUGR alone (Table 4).

## Discussion

Our present study demonstrates that the 15-month-old male IUGR offspring develops hyperglycemia, glucose intolerance with reduced GSIS in the first and second phases of IVGTT, unsuppressed HGP, and a reduction of total-body GC. Although circulating baseline insulin concentrations are within normal limits, these glucose/insulin metabolic perturbations are consistent with inadequate pancreatic $\beta$-cell secretion of insulin in response to an exogenous glucose load. Previous investigations early in life at PN21 revealed a reduction in $\beta$-cell fractional area and mass due to inadequate replication in the IUGR (30). At 15

**TABLE 3.** Mean ± SEM for the plasma lipid profile for all groups (milligrams per deciliter) and plasma lipid-corrected values for the AIR obtained 5 min after iv glucose injection

| | CON (6) | IUGR (6) | IPGR (6) | PNGR (6) |
|---|---|---|---|---|
| Triglycerides | 88.5 ± 12 | 113.2 ± 19.9 | 101.3 ± 6.1 | 113.8 ± 10.3 |
| Triglycerides/AIR | 16.1 ± 3.1 | 63.5 ± 32.6[a,b,c] | 14.9 ± 2.1[d] | 14 ± 2.8[d] |
| Total cholesterol | 102.3 ± 5.9 | 105.2 ± 11.1 | 107.2 ± 4.6 | 108.7 ± 7.1 |
| Total cholesterol/AIR | 18.8 ± 3.0 | 48.7 ± 18.9[a,b,c] | 15.3 ± 1.0[d] | 13.5 ± 2.6[d] |
| HDL | 50.2 ± 3.8 | 50.4 ± 4.4 | 51.8 ± 2.9 | 50.7 ± 3.9 |
| HDL/AIR | 9.0 ± 1.2 | 22.7 ± 8.2[a,b,c] | 7.4 ± 0.4[d] | 6.3 ± 1.2[d] |
| UC | 27.2 ± 1.6 | 27.6 ± 3.3 | 29.3 ± 1.3 | 28.3 ± 1.8 |
| UC/AIR | 5.0 ± 0.7 | 12.4 ± 4.8[a,b,c] | 4.2 ± 0.2[d] | 3.5 ± 0.6[d] |
| FFA | 8.3 ± 1.6 | 8.4 ± 1 | 7.7 ± 0.8 | 7.3 ± 0.6 |
| FFA/AIR | 1.4 ± 0.2 | 3.9 ± 1.6[a,b,c] | 1.1 ± 0.1[d] | 0.9 ± 0.1[d] |

Number of animals for each parameter is shown in parentheses (n). FFA, Free fatty acids.

[a] $P < 0.05$ all groups *vs.* CON.

[b] $P < 0.05$ *vs.* IPGR.

[c] $P < 0.05$ *vs.* PNGR.

[d] $P < 0.05$ *vs.* IUGR.

months of age, as seen in our present study, a trend toward a reduction in β-cell fractional area and mass persists in the IUGR adult offspring, consistent with development of perturbed GSIS.

Hyperglycemia at 15 months of age supports the onset of pancreatic β-cell functional failure. In addition, the inadequate suppression of HGP along with diminished total-body GC supports the presence of insulin resistance, seen as reduced $S_I$ in the IUGR adult offspring. The calculated DI reveals that a trend toward reduced $S_I$ is associated with reduced insulin secretion in the IUGR adult offspring, rather than the necessary increase that is required to overcome the reduced insulin sensitivity. However, our studies did not show any decrease in liver or WAT IR concentrations in the IUGR adult offspring because the resistive block may reside in a postreceptor step, namely activation of protein kinase Cζ as seen previously (27). Furthermore, although no change in either the high-capacity, low-affinity hepatic Glut2 (Michaelis constant = 15–20 mM) or WAT total Glut1 (basal) or Glut4 (requires association with plasma membrane for transporting glucose) concentrations was evident, an increase in hepatic Glut1 concentrations that existed in the IUGR adult offspring, may signify enhanced intrahepatic glucose transport in the presence of hyperglycemia.

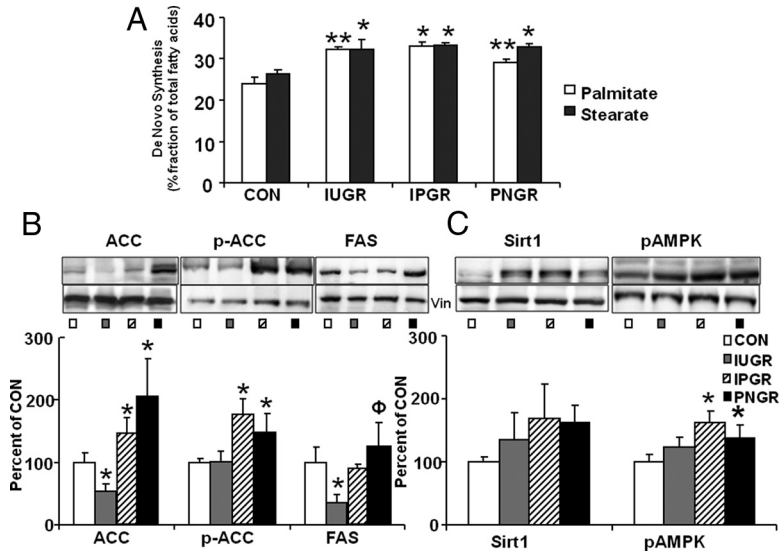


**FIG. 4.** *De novo* lipogenesis and hepatic lipid metabolizing enzymes and markers of energy state. A, *De novo* lipogenesis. The fraction of newly synthesized palmitate (c16:0) and stearate (c18:0) is shown as percentage of total fatty acids determined from isotopically labeled [2-$^2$H]fatty acids by mass isotopomer distribution analysis (MIDA) in CON (n = 6), IUGR (n = 5), IPGR (n = 6), and PNGR (n = 6). **, $P < 0.0001$ *vs.* CON; *, $P < 0.002$ *vs.* CON. B, Hepatic enzyme expression. ACC, p-ACC, and FAS (*upper panels*) that increase DNL are depicted in representative Western blots with vinculin (*lower panels*) as the internal control within the *inset*. The quantification is seen as a bar graph below in arbitrary units presented as a percentage of the CON value (n = 6 for each enzyme and each group). *, $P < 0.05$ *vs.* CON; ϕ, $P < 0.05$, IUGR *vs.* PNGR. C, Hepatic expression of Sirt1 and pAMPK (*upper panels*) that decrease DNL is depicted with vinculin (Vin; *lower panel*) as the internal control in representative Western blots within the *inset*. The quantification is seen as a bar graph below in arbitrary units presented as a percent of the CON value (n = 6 for each protein and each group). *, $P < 0.05$ *vs.* CON.

Our previous investigations at an earlier stage in the 10-month-old IUGR male offspring revealed significant sc and visceral adiposity without hyperglycemia or glucose intolerance. Furthermore, after exogenous insulin administration under hyperinsulinemic-euglycemic clamp conditions, the male obese, glucose-tolerant IUGR male offspring (4) was insulin sensitive rather than insulin resistant. The question remained whether insulin sensitivity in the adult male IUGR reflected persistence of metabolic programming secondary to prenatal

**TABLE 4.** WAT gene expression profile

| | CON (6) | IUGR (6) | IPGR (6) | PNGR (6) |
|---|---|---|---|---|
| Genes mediating fatty acid transport and synthesis | | | | |
| FAS | 100.0 ± 3.1 | 95.9 ± 12.1 | 79.5 ± 6.7 | 95.9 ± 13.5 |
| FATP1 | 100 ± 8.3 | 151.6 ± 18.2[a,b,c] | 51.1 ± 5.0[a,d] | 54.9 ± 6.1[a,d] |
| FOXO1 | 100 ± 5.8 | 119.3 ± 10.4[b,c] | 47.5 ± 3.6[a,d] | 39.6 ± 4.0[a,d] |
| ACC$\alpha$ | 100.0 ± 2.8 | 100.0 ± 5.5[b,c] | 39.3 ± 2.1[a,d] | 56.0 ± 4.2[a,d] |
| PPAR$\gamma$ | 100.0 ± 7.12 | 123.4 ± 5.4[a,b,c] | 72.3 ± 4.6[a,d] | 82.3 ± 5.7[a,d] |
| SREBP1 | 100.0 ± 3.3 | 132.5 ± 9.3 | 98.6 ± 12.1 | 98.2 ± 10.0 |
| SREBP2 | 100 ± 7.01 | 92.7 ± 9.1 | 94.1 ± 7.2 | 122.4 ± 18.4 |
| Factors associated with fatty acid synthesis | | | | |
| Sirt1 | 100 ± 4.8 | 96.6 ± 6.2 | 67.6 ± 4.7[a,d] | 61.4 ± 10.8[a,d] |
| SCD1 | 100.0 ± 16.8 | 127.9 ± 28.3 | 131.9 ± 20.6 | 185.2 ± 33.9 |
| RBP4 | 100.0 ± 7.9 | 108.1 ± 10.7[b,c] | 55.1 ± 3.7[a,d] | 58.7 ± 9.2[a,d] |
| Adipokines | | | | |
| Resistin | 99.8 ± 7.4 | 165.5 ± 12.1[a,b] | 118.7 ± 2.2[d] | 150.7 ± 6.9[a] |
| Visfatin | 100.0 ± 5.4 | 312.1 ± 72.1[a] | 232.9 ± 21.6 | 281.5 ± 21.3[a] |
| Leptin | 99.8 ± 7.2 | 108.2 ± 5.3[b] | 180.5 ± 18.5[a,d] | 137.8 ± 3.0[a] |
| Adiponectin | 100.0 ± 4.7 | 125.7 ± 18.8 | 118.5 ± 8.4 | 108.8 ± 22.6 |
| TNF$\alpha$ | 100.0 ± 14.4 | 163.4 ± 30.2 | 121.9 ± 23.3 | 121.8 ± 20.8 |
| Adiponutrin | 100 ± 6.7 | 116.2 ± 6.8[b,c] | 65.0 ± 5.2[a,d] | 72.0 ± 6.78[a,d] |

All data are shown as mean ± SEM, expressed as a percentage of the CON value, and the numbers in *parentheses* represent n for each gene.
[a] $P < 0.05$ all groups *vs.* CON.
[b] $P < 0.05$ *vs.* IPGR.
[c] $P < 0.05$ *vs.* PNGR.
[d] $P < 0.05$ *vs.* IUGR.

caloric restriction or rather the subsequent emergence of insulin resistance with further advancement in age that was not yet evident at this stage. Our present investigation carried out at 15 months of age using stable isotopes allowed quantification of glucose kinetics under conditions of endogenous insulin secretion. Under these circumstances, characteristics of insulin resistance emerged, in keeping with deficient insulin secretion. Although not reflected in total WAT Glut4 concentrations in our study, insulin resistance was previously evident in the insulin resistance of plasma membrane-associated Glut4 concentrations (28). Alternatively, the lack of adequate endogenous insulin secretion can lift suppression of HGP and reduce GC (utilization). Nevertheless, these perturbations collectively result in glucose intolerance at 15 months, unlike the glucose-tolerant state seen at 10 months of age in the adult male IUGR offspring (4). Therefore, obesity ensues chronologically earlier at 10 months or before than glucose intolerance, which emerges at 15 months in the adult male IUGR offspring. These investigations in males when compared with our prior investigations in 15-month-old females reveal an overt phenotype of metabolic derangement in males, whereas females reveal dysregulation of HGP (14) alone. Moreover, females when pregnant demonstrate gestational hyperglycemia (31), perhaps related to $\beta$-cell failure, unmasked during pregnancy induced insulin-resistant state.

At 15 months of age in males, the presence of obesogenic features with hyperglycemia and glucose intolerance sets the stage for development of type 2 diabetes mellitus with associated hyperphagia and a tendency toward polydipsia. Under these conditions, DNL increased substantially in the IUGR, perhaps as a result of postreceptor insulin resistance and hyperglycemia. Increased hepatic Glut1 concentrations and thereby function may have fueled enhanced DNL. Thus, changes in GSIS, HGP, and GC along with DNL may serve as predictors of type 2 diabetes and dyslipidemia, both of which are major risk factors for coronary artery disease, stroke, and death.

Hepatic ACC and fatty acid synthase, key enzymes necessary for increasing DNL, were reduced, but with associated dyslipidemia related to diminished GSIS, in the adult IUGR offspring, being consistent with previous observations in obese human subjects (32). This suggests that the observed enhanced DNL in the IUGR male offspring may be adaptive toward achieving basal eulipidemia or maladaptive causing dyslipidemia when GSIS is reduced in the adult IUGR offspring. Alternatively, this adaptive response may reflect prior exposure to prenatal caloric restriction rather than adult-onset hyperglycemia and insulin resistance. Thus, one scenario could be that prenatal

caloric restriction with IUGR prompts the cascade of compensatory hepatic DNL upon postnatal exposure to adequate caloric intake. This adaptive enhanced DNL may have set early in life persisting into adulthood. Because we did not measure DNL in early life, we can only speculate on this nutritional programming effect seen in the IUGR adult offspring. The fact that adult IUGR hepatic ACC and FAS, mediators of lipogenesis, were suppressed, incongruent with enhanced DNL lends support to this speculation.

Furthermore, this suppression of hepatic lipogeneic enzymes are reflective of defective GSIS. Adequate amounts of insulin secretion is necessary to stimulate hepatic lipogeneic enzymes, thereby driving glucose into the lipogenic pathway. The lack of required amounts of GSIS may be responsible for reduced hepatic ACC and FAS protein expression in the adult offspring. Thus, these observations cumulatively support enhanced DNL in the adult IUGR offspring to not be due to adult acquisition of reduced GSIS induced suppressed hepatic fatty acid-synthesizing enzymes, but rather the remnant or persistence of an adaptation instituted early in life in response to nutritional perturbations, a form of programming.

In IUGR the visceral WAT demonstrates an increase in resistin, visfatin, and *FATP1* gene expression in particular. These findings support enhanced fatty acid transport and synthesis, thereby reflecting skeletal muscle insulin resistance as described by us (28) and other investigators (29, 33, 34). Enhanced WAT fatty acid transport and synthesis is not reflected by increased visceral WAT amounts and circulating leptin concentrations *vs.* CON at 15 months, but visceral and sc adiposity is noted at 10 months of age (4). However, the 15-month male IUGR adult offspring are heavier with larger livers, reflecting fatty livers, and perhaps accumulating sc and maldistributed fat within various tissues. Thus, these changes in visceral WAT gene expression may either reflect remnants of prior obesity or the present obesogenic tendency in the IUGR adult offspring.

PNGR adult males demonstrate no change in circulating glucose or insulin concentrations, no effect on GSIS overall but hyperinsulinemia noted in the first 5 min of the exogenous glucose load, and no change in HGP but an increase in GC. These findings support the previous observation earlier in life that demonstrated no change in pancreatic $\beta$-cell mass but rather a reduction in exogenous pancreatic mass (30). In addition, no sign of insulin resistance but rather an enhanced insulin-sensitive state was evident in our present study. Reflecting the normal ability to secrete insulin in response to an exogenous glucose load along with hyperinsulinemia is the enhanced hepatic ACC, pACC, and FAS protein concentrations. However, similar to the IUGR adult offspring, the 15-month-old lean male PNGR offspring also revealed greater hepatic Glut1 concentrations despite the lack of hyperglycemia, paralleling increased DNL related to increased palmitate and stearate synthesis, despite the lack of dyslipidemia.

These changes in DNL also occur in the face of increased hepatic pAMPK, reflective of a cellular energy-deficient state that is known to suppress DNL, again supporting the possibility of a permanency of the adaptive increase in DNL in response to early life (postnatal) calorie restriction rather than a predictor of obesity. This speculation is further supported by the reduced visceral WAT content and circulating leptin concentrations seen in the adult PNGR offspring. In keeping with this observation is the reduction in visceral WAT Sirt1, FOXO1, ACC$\alpha$, RBP4, adiponutrin, PPAR$\gamma$, and FATP1 but an increase in visfatin expression in the PNGR adult offspring. Many of these down-regulated factors and enzymes suggest reduced fatty acid transport and synthesis or reflect WAT insulin resistance. Thus, unlike the IUGR adult offspring, the adult PNGR offspring was lean and insulin sensitive ($S_I$ similar to CON) and exhibited an adaptive increase in DNL.

When the insulin-sensitive state of PNGR was superimposed on the insulin-deficient/insulin-resistant state of IUGR, it led to enhanced GSIS during the first 5 min, albeit culminating in a normal insulin-responsive state akin to that of CON. This consisted of no observed change in GSIS, HGP, or GC. Thus, for the most part, the IPGR exhibited metabolic features that were in between that seen in the IUGR and PNGR adult offspring. Although IPGR was lean, akin to PNGR, the match between the intrauterine and postnatal nutritional environments in the IPGR protected the IUGR from exposure to mismatched intrauterine and postnatal nutritional environments. Furthermore, superimposition of PNGR on IUGR offered added protection from diabetic and obesogenic features. This may be due to the increased pancreatic $\beta$-cell area and mass and enhanced insulin sensitivity that collectively translate into a higher DI. Peripherally, increased WAT IR reflects this insulin-sensitive state. IPGR, similar to PNGR and IUGR, revealed increased hepatic Glut1 and enhanced DNL, an adaptation responding to early-life caloric restriction.

However, similar to PNGR, IPGR exhibited increased hepatic ACC and pACC, with normal FAS protein concentrations reflecting the normalization of adult GSIS from that of the IUGR. Furthermore, increased hepatic pAMPK concentrations were consistent with a hepatic cellular energy deficit akin to PNGR. Unlike IUGR but mimicking PNGR, a reduction in visceral WAT Sirt1, FOXO1, ACC$\alpha$, RBP4, adiponutrin, PPAR$\gamma$, and FATP1 and an increase in visfatin expression were noted, consistent with

reduced visceral WAT content and circulating leptin concentrations. Thus, superimposition of PNGR on IUGR normalized the maladaptive adult phenotype of the latter. The fact that IPGR is able to protect against the glucose-intolerant, insulin-resistant, and obesogenic-presenting phenotype of the adult IUGR offspring but not against the adaptive enhanced DNL that parallels increased hepatic Glut1 favors augmented DNL as a biomarker of an early life event, namely caloric restriction in our present study. Thus, early life caloric restriction, both prenatal and postnatal, appears to program elevated DNL, which persists into the *ad libitum*-feeding adult offspring. This adaptive enhanced DNL may be necessary to maintain a normal basal circulating lipid profile in all three early caloric restriction groups. Thus, enhanced DNL is more sensitive an indicator than perturbed circulating lipid profile in the basal state because the latter reciprocally reflects the adult acute insulin response to an exogenous glucose load.

Our investigations measured palmitate and stearate synthesis based on deuterium incorporation. The dietary macronutrient composition and caloric density along with food intake per gram body weight between the different experimental groups were similar after weaning onward and during these studies. Additionally, the deuterium enrichment was similar in all four groups. Hence, the observed changes in DNL represent adaptations restricted to early changes in dietary fat and carbohydrate content encountered only during prenatal and/or postnatal life.

In summary, the male adult IUGR offspring subjected to a mismatch between prenatal caloric restriction and postnatal unrestricted food intake develops hyperglycemia and glucose intolerance, signifying diabetic with certain obesogenic features. In addition, insufficient GSIS and peripheral insulin action reflecting insulin resistance is evident. Although one can conjecture that overt diabetes exists related to features of hyperphagia and polydipsia in the presence of hyperglycemia and glucose intolerance, the IUGR offspring is at increased risk of developing various life-threatening complications if exposed to hypercaloric diets during postnatal life. It is also possible that exogenous insulin administration by itself or in the context of a hyperinsulinemic-euglycemic clamp in the 15-month-old adult male IUGR offspring could overcome the encountered insulin deficiency and insulin resistance, thereby ameliorating the present situation as previously reported in aging IUGR male offspring (35). However, superimposition of sufficient insulin-producing and insulin-sensitive lean PNGR on IUGR protects the latter from diabetes and obesogenic features (4). Unique to these observations is the enhanced DNL paralleling increased hepatic Glut1 concentrations in IUGR, PNGR, and IPGR adult male offspring with varied adult phenotypes but with the common denominator of early life caloric restriction.

## Acknowledgments

We thank Shanthie Thamotharan and Bo-Chul Shin, Ph.D., for assistance with tissue and plasma collection and with some Western blot analyses.

Address all correspondence and requests for reprints to: Sherin U. Devaskar, M.D., or Meena Garg, M.D., Department of Pediatrics, Division of Neonatology and Developmental Biology, Neonatal Research Center, University of California, Los Angeles, 10833 Le Conte Avenue, MDCC-22-402, Los Angeles, California 90095-1752. E-mail: sdevaskar@mednet.ucla.edu; or mgarg@mednet.ucla.edu.

This work was supported by Grants HD-41320 and HD-25024 from the National Institutes of health (to S.U.D.).

Disclosure Summary: The authors have nothing to disclose.

## References

1. **Barker DJ** 2001 The malnourished baby and infant. Br Med Bull 60:69–88
2. **Barker DJ, Hales CN, Fall CH, Osmond C, Phipps K, Clark PM** 1993 Type 2 (non-insulin-dependent) diabetes mellitus, hypertension and hyperlipidaemia (syndrome X): relation to reduced fetal growth. Diabetologia 36:62–67
3. **Petersen KF, Dufour S, Savage DB, Bilz S, Solomon G, Yonemitsu S, Cline GW, Befroy D, Zemany L, Kahn BB, Papademetris X, Rothman DL, Shulman GI** 2007 The role of skeletal muscle insulin resistance in the pathogenesis of the metabolic syndrome. Proc Natl Acad Sci USA 104:12587–12594
4. **Garg M, Thamotharan M, Dai Y, Thamotharan S, Shin BC, Stout D, Devaskar SU** 2012 Early postnatal caloric restriction protects adult male intrauterine growth-restricted offspring from obesity. Diabetes 61:1391–1398
5. **Burns SP, Desai M, Cohen RD, Hales CN, Iles RA, Germain JP, Going TC, Bailey RA,** 1997 Gluconeogenesis, glucose handling, and structural changes in livers of the adult offspring of rats partially deprived of protein during pregnancy and lactation. J Clin Invest 100:1768–1774
6. **Postic C, Girard J** 2008 The role of the lipogenic pathway in the development of hepatic steatosis. Diabetes Metab 34(6 Pt 2):643–648
7. **Desai M, Babu J, Ross MG** 2007 Programmed metabolic syndrome: prenatal undernutrition and post-weaning overnutrition. Am J Physiol Regul Integr Comp Physiol 293:R2306–R2314
8. **Hudgins LC, Hellerstein M, Seidman C, Neese R, Diakun J, Hirsch J** 1996 Human fatty acid synthesis is stimulated by a eucaloric low fat, high carbohydrate diet. J Clin Invest 97:2081–2091
9. **Musso G, Gambino R, Cassader M** 2009 Recent insights into hepatic lipid metabolism in non-alcoholic fatty liver disease (NAFLD). Prog Lipid Res 48:1–26
10. **Rodgers JT, Puigserver P** 2007 Fasting-dependent glucose and lipid metabolic response through hepatic sirtuin 1. Proc Natl Acad Sci USA 104:12861–12866
11. **Purushotham A, Schug TT, Li X** 2009 SIRT1 performs a balancing act on the tight-rope toward longevity. Aging (Albany, NY) 1:669–673
12. **Li Y, Xu S, Mihaylova MM, Zheng B, Hou X, Jiang B, Park O, Luo**

**Z, Lefai E, Shyy JY, Gao B, Wierzbicki M, Verbeuren TJ, Shaw RJ, Cohen RA, Zang M** 2011 AMPK phosphorylates and inhibits SREBP activity to attenuate hepatic steatosis and atherosclerosis in diet-induced insulin-resistant mice. Cell Metab 13:376–388

13. **Strable MS, Ntambi JM** 2010 Genetic control of *de novo* lipogenesis: role in diet-induced obesity. Crit Rev Biochem Mol Biol 45: 199–214
14. **Garg M, Thamotharan M, Rogers L, Bassilian S, Lee WN, Devaskar SU** 2006 Glucose metabolic adaptations in the intra-uterine growth restricted adult female rat offspring. Am J Physiol Endocrinol Metab 290:E1218–E1226
15. **Lowenstein JM, Brunengraber H, Wadke M** 1975 Measurement of rates of lipogenesis with deuterated and tritiated water. Methods Enzymol 35:279–287
16. **Szafranek J, Pfaffenberger CD, Horning EC** 1974 The mass spectra of some per-*O*-acetylaldononitriles. Carbohydr Res 38:97–105
17. **Xu J, Lee WN, Xiao G, Trujillo C, Chang V, Blanco L, Hernandez F, Chung B, Makabi S, Ahmed S, Bassilian S, Saad M, Kurland IJ** 2003 Determination of a glucose-dependent futile recycling rate constant from an intraperitoneal glucose tolerance test. Anal Biochem 315:238–246
18. **Lee WN, Byerley LO, Bergner EA, Edmond J** 1991 Mass isotopomer analysis: theoretical and practical considerations. Biol Mass Spectrom 20:451–458
19. **Xu J, Chang V, Joseph SB, Trujillo C, Bassilian S, Saad MF, Lee WN, Kurland IJ** 2004 Peroxisomal proliferator-activated receptor $\alpha$ deficiency diminishes insulin-responsiveness of gluconeogenic/glycolytic/pentose gene expression and substrate cycle flux. Endocrinology 145:1087–1095
20. **Lee WN, Bassilian S, Guo Z, Schoeller D, Edmond J, Bergner EA, Byerley LO** 1994 Measurement of fractional lipid synthesis using deuterated water ($2H_2O$) and mass isotopomer analysis. Am J Physiol 266(3 Pt 1):E372–E383
21. **Lee WN, Bassilian S, Lim S, Boros LG** 2000 Loss of regulation of lipogenesis in the Zucker diabetic (ZDF) rat. Am J Physiol Endocrinol Metab 279:E425–E432
22. **Bassilian S, Ahmed S, Lim SK, Boros LG, Mao CS, Lee WN** 2002 Loss of regulation of lipogenesis in the Zucker diabetic rat. II. Changes in stearate and oleate synthesis. Am J Physiol Endocrinol Metab 282:E507–E513
23. **Puppione DL, Charugundla S** 1994 A microprecipitation technique suitable for measuring $\alpha$-lipoprotein cholesterol. Lipids 29:595–597
24. **Warnick GRE** 1986Enzymatic methods for quantification of lipoprotein lipids. In: Segrest JP, Albers JJ, eds. Methods in enzymology. Vol 129. New York: Academic; 101-12325.
25. **Faerch K, Brons C, Alibegovic AC, Vaag A** The disposition index: adjustment for peripheral vs. hepatic insulin sensitivity? J Physiol 588(Pt 5):759–764
26. **Shin BC, McKnight RA, Devaskar SU** 2004 Glucose transporter GLUT8 translocation in neurons is not insulin responsive. J Neurosci Res 75:835–844
27. **Oak SA, Tran C, Pan G, Thamotharan M, Devaskar SU** 2006 Perturbed skeletal muscle insulin signaling in the adult female intrauterine growth-restricted rat. Am J Physiol Endocrinol Metab 290: E1321–E1330
28. **Thamotharan M, Shin BC, Suddirikku DT, Thamotharan S, Garg M, Devaskar SU** 2005 GLUT4 expression and subcellular localization in the intrauterine growth-restricted adult rat female offspring. Am J Physiol Endocrinol Metab 288:E935–E947
29. **Choi GY, Tosh DN, Garg A, Mansano R, Ross MG, Desai M** 2007 Gender-specific programmed hepatic lipid dysregulation in intrauterine growth-restricted offspring. Am J Obstet Gynecol 196: 477.e1–e7
30. **Matveyenko AV, Singh I, Shin BC, Georgia S, Devaskar SU** 2010 Differential effects of prenatal and postnatal nutritional environment on ss-cell mass development and turnover in male and female rats. Endocrinology 151:5647–5656
31. **Garg M, Thamotharan M, Pan G, Lee PW, Devaskar SU**2010 Early exposure of the pregestational intrauterine and postnatal growth-restricted female offspring to a peroxisome proliferator-activated receptor-$\gamma$ agonist. Am J Physiol Endocrinol Metab 298:E489–E498
32. **Ortega FJ, Mayas D, Moreno-Navarrete JM, Catalán V, Gómez-Ambrosi J, Esteve E, Rodriguez-Hermosa JI, Ruiz B, Ricart W, Peral B, Fruhbeck G, Tinahones FJ, Fernández-Real JM** The gene expression of the main lipogenic enzymes is downregulated in visceral adipose tissue of obese subjects. Obesity (Silver Spring) 18:13–20
33. **Desai M, Guang Han, Ferelli M, Kallichanda N, Lane RH** 2008 Programmed upregulation of adipogenic transcription factors in intrauterine growth-restricted offspring. Reprod Sci 15:785–796
34. **Magee TR, Han G, Cherian B, Khorram O, Ross MG, Desai M** 2008 Down-regulation of transcription factor peroxisome proliferator-activated receptor in programmed hepatic lipid dysregulation and inflammation in intrauterine growth-restricted offspring. Am J Obstet Gynecol 199:271.e1–e5
35. **Dai Y, Thamotharan S, Garg M, Shin BC, Devaskar SU** 2012 Superimposition of postnatal calorie restriction protects the aging male intrauterine growth-restricted offspring from metabolic maladaptations. Endocrinology 153:4216–4226